Quantum theory of atomic position measurement using optical fields

J. E. Thomas
Department of Physics, Duke University, Durham, North Carolina 27706
(Received 23 February 1990; revised manuscript received 11 June 1990)

A simple quantum theory of recently suggested optical techniques for ultrahigh-resolution position measurement and localization of moving atoms in beams is presented. Both the internal and center-of-mass motion are treated quantum mechanically so that the limitations on the ultimate position resolution due to atomic motion and wave-mechanical diffraction are included in the analysis. The techniques utilize a miniaturized form of Raman-induced resonance imaging in which optical fields are used to make transitions from a long-lived initial state to a long-lived final state. The final state is shifted by the spatially varying potential of an applied force field in order to correlate the atomic position with its resonance frequency. Spatially varying level shifts are obtainable by using very large Zeeman field gradients or spatially varying light shifts in a small interaction volume. This results in very high spatial resolution. The atomic transit time across the optical-field region is limited by focusing to an ideal diameter that minimizes the spatial resolution length. The results of the analysis show that nanometer spatial resolution of the initial-state position distribution is attainable. Under appropriate conditions, the final-state spatial wave function can take the form of a minimum-uncertainty Gaussian wave packet obeying $\Delta x \Delta p = \hbar/2$. Such states may prove useful in studying one-dimensional wave-packet motion in applied potentials.

I. INTRODUCTION

Recently there has been substantial progress and interest in the creation of atomic distributions which vary over small length scales. In atomic beams, such distributions arise by diffraction,[1] periodic spatial modulation,[2] channeling,[3] focusing,[4] and cooling.[5] In general, the distributions exhibit momentum-space coherence and are of both practical and fundamental interest. These developments have been spurred on, in part, by the advent of practical laser-cooling techniques.[6] Important applications include atomic interferometry, gyroscopes, and the creation of submicrometer structures by atomic deposition.[1,2]

While techniques exist to create suboptical-wavelength atomic spatial modulation and interference in atomic beams, methods for detection have been limited principally to hot wires. Only in Ref. 3 is optical absorption used to determine the atomic position distribution. In that work, atoms are channeled in an off-resonant optical standing wave. Due to the spatial variation of the light shifts in the standing wave, atoms at a node resonate at a different frequency than atoms at a peak in the optical field. Thus, a two-peak absorption spectrum is obtained in which the height and shape of the peaks vary when the atoms are redistributed by channeling, compared to when they are not channeled. Since the channeling field and the spatially varying light shift which causes the channeling vary with the same scale of length, the true periodic structure of the channeled atomic distribution could not be directly measured in the experiments. While the position resolution obtained was adequate (although not specified in Ref. 3), it was limited by the spontaneous linewidth for the transition employed as well as by Doppler broadening. Further, the diameter of the interaction region (4.6 mm) was chosen to achieve channeling without heating. In this case, the interaction time is long enough for the atoms to be redistributed over distances comparable to an optical wavelength. For optimum position resolution, our calculations show that the interaction time of the atoms with the measurement field must be much shorter, since the atoms must move no more than the optimum resolution length. This is much shorter than an optical wavelength for the large light shifts employed in the experiments.

The purpose of this paper is to analyze a recently suggested class of techniques[7] which may prove useful in achieving much higher spatial resolution of moving atoms using optical fields than has been obtained previously. We begin by reviewing the principal features of the method using heuristic arguments and then proceed to the detailed derivation.

The basic method, Fig. 1, is to use a spatially varying potential $V(x)$, which makes the resonance frequency of simple atoms position dependent, analagous to magnetic resonance (MR) imaging. Unlike conventional MR imaging, the proposed method employs Raman-induced resonance imaging using optical fields. The use of optical fields permits the measurements to be made in very small volumes with very large spatially varying potentials, which leads to quantum-mechanical limits on the ultimate measurement accuracy. As shown in Fig. 1, the atoms enter the Raman interaction region in a long-lived initial state (i) which is *not* shifted by the potential $V(x)$ and make a transition via two optical fields to a long-lived final state (f) which is shifted by the applied potential. In this way, the atomic position and its resonance frequency are correlated. The total number of atoms emerging in the final state is measured downstream from the Raman region. This signal is proportional to the number of atoms in the initial state which make a transition to the final state near the position where the optical fields

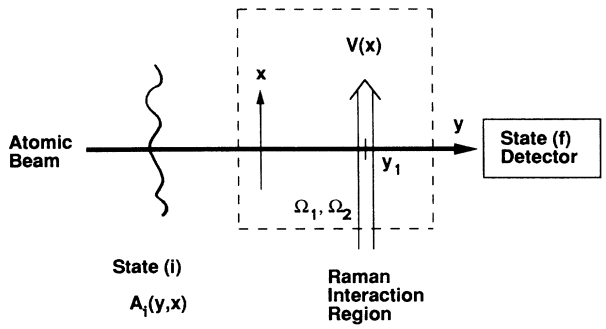

FIG. 1. Atomic-position measurement by Raman-induced resonance imaging. Atoms enter the Raman interaction region in an initial state i with some spatial distribution along the measurement axis x which is to be measured. The initial-state amplitude $A_i(y,x)$ is presumed to be specified at the plane $y=y_1$ centered in the Raman fields Ω_1,Ω_2. A spatially varying potential $V(x)$ shifts the final state f without affecting the initial state i and correlates the Raman resonance frequency with the atomic position along the x axis. Atoms which are detected downstream in state f are those which have made the $i\rightarrow f$ transition in a narrow spatial region Δx where the Raman fields are resonant for the $i\rightarrow f$ transition.

are resonant with the Raman transition. The goal is to measure prepared *incident* atomic distributions without modification due to trapping or channeling, by appropriately limiting the interaction time. These techniques examine interesting features of quantum-mechanical position measurement and should make it possible to localize atoms to much better than an optical wavelength for application to a variety of interesting experiments. For the ^{154}Sm or ^{174}Yb systems we are currently studying, it should be possible to achieve position resolution of $\simeq 70$ Å.

An important feature of the analysis is that it determines the ultimate spatial resolution attainable for *moving* atoms in large spatially varying level shift gradients which correlate the atomic resonance frequency with position. The results should have important bearing on experiments which measure the interaction of atoms with surfaces.[8]

Finally, it is shown below that the center-of-mass wave function for atoms which emerge in the final state is highly localized and, under appropriate conditions, can take the form of a minimum uncertainty Gaussian wave packet. These results complement recent work on atomic and molecular internal state wave packets.[9]

For optimum position resolution, it is necessary that both radiative and Doppler broadening, as well as the laser linewidth, be negligible compared to transit-time broadening. In some cases, a one-photon transition from the ground state is adequate. This would require a long-lived excited state, large spatially varying level shifts, and high atomic-beam collimation. Alternatively, a Raman-induced resonance between long-lived ground states can be used,[7] as mentioned above and described below.

To explain the Raman-induced resonance imaging method in more detail, suppose that an atomic beam is prepared in an initial long-lived internal state (i) with some interesting spatial distribution perpendicular to the atomic-beam propagation axis. To measure the spatial distribution, the atoms enter an interaction region containing two optical fields of frequencies Ω_1,Ω_2 which can induce Raman transitions between the long-lived initial state and a long-lived final state f. The interaction region also contains a spatially varying potential which makes the Raman resonance frequency dependent on the spatial position of the atom. For simplicity, suppose that the spatially varying potential is due to a uniform force F which affects only the final state (f) of the atom. The potential is taken to vary linearly along the x axis, which is perpendicular to the atomic-beam propagation direction, and which ultimately will become the measurement axis. For concreteness, let x_0F be the shift of the final state due to a uniform Zeeman field, and $-xF$ be the shift of the final state due to an additional Zeeman shift or light shift which varies linearly in space. The net potential can be written as

$$V(x-x_0)=-(x-x_0)F\ . \tag{1}$$

Further, suppose that the atoms which enter this potential in the internal state (i) are *not* shifted. In this case, the i-f resonance frequency varies linearly in space, so that a resonance field of sufficient frequency resolution can cause $i\rightarrow f$ transitions in a highly localized region Δx along the x axis. The position resolution Δx is determined by the potential-energy change $\Delta V=F\Delta x$ and the frequency resolution $\Delta\omega$ according to

$$\frac{F}{\hbar}\Delta x=\Delta\omega\equiv\frac{1}{T^*}\ , \tag{2}$$

where T^* is the effective interaction time which determines the frequency resolution. If a one-photon optically allowed transition is employed, then the frequency resolution will be limited by Doppler and radiative broadening as well as by laser-frequency jitter. All of these deficiencies are remedied by using a copropagating-wave Raman-induced resonance between long-lived states (i) and (f) via some off-resonant intermediate state (I) as shown in Fig. 2.

The optical fields Ω_1,Ω_2 are taken to copropagate. By choice of the difference frequency $\Omega_2-\Omega_2$, a Raman resonance with the $i\rightarrow f$ transition frequency ω_{fi} can be made to occur at the point $x=x_0$ along the measurement axis. The Raman fields are derived by A/O modulation from the laser field ω so that the difference frequency is easily made very stable. By using an off-resonant Raman transition and copropagating fields, the laser jitter, beam divergence, Doppler shifts, etc., drop out, since only the difference frequency enters. This technique was employed previously to obtain Raman-induced Ramsey resonances using optical fields, where 100-Hz resolution was readily obtained.[10] By monitoring the total count rate of atoms in state f emerging from the Raman region versus uniform Zeeman shift (which varies x_0), the incident spatial distribution in state i is determined. Only initial state atoms near $x=x_0$, the point at which $\Omega_1-\Omega_2=\omega_{fi}$, contribute to the signal.

The use of optical fields in the measurement leads to a

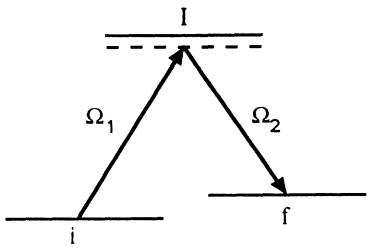

FIG. 2. Level scheme and Raman fields.

number of new features which are listed briefly here.

(1) *Spatially Varying Level Shifts.* Two-wire magnetic-field gradients as developed for atom-deflection applications can be used to achieve spatially varying level shifts $F/h = 10^{10}$ Hz/cm over millimeter length scales. Over smaller maximum distances, very large spatially varying level shifts can be obtained by using the light shifts of intense, nonresonant intersecting laser beams (*not* the Raman beams). In this case, more than 10^{12} Hz/cm is feasible. Spatially varying shifts this large have been used in atom-channeling experiments, but application to position measurements which yield the incident spatial distribution have not been explored. When the interaction time is optimally limited as described below, exceedingly high spatial resolution is attainable.

(2) *Spatial Resolution.* When long-lived states (i,f) are chosen for measurement, the interaction time T^* is determined by the atom transit time T across the Raman region. In this case, the use of optical fields allows the interaction time to be limited to an optimum value by focusing. The optimum value of T is determined by the criterion that the atom not move across the ideal resolution length during the measurement. The simplest limit is due to the atomic velocity component v_x along the measurement axis. In this case, the optimum interaction time is $T=\Delta x/v_x$. With Eq. (2), the optimum spatial resolution is given by

$$\Delta x_{\rm vel}=\sqrt{\hbar v_x/F}\ . \tag{3}$$

For modest atomic-beam collimation and a two-wire magnetic-field gradient, *suboptical-wavelength* position resolution is readily attainable.

For a highly collimated atomic beam, v_x no longer limits the interaction time. In this case, the acceleration due to the applied force and diffraction out of the resolution length limit the smallest regions which are measurable. For the acceleration limit, the optimum value of the interaction time is such that $(F/2M)T^2=\Delta x$. For the diffraction limit, the interaction time must be such that a particle localized into a region of length Δx spread only over distances comparable to Δx, i.e., $(\hbar/2M\Delta x)T=\Delta x$. In either case, with Eq. (2), the optimum resolution is

$$\Delta x_{\rm accel}=\left[\frac{\hbar^2}{2MF}\right]^{1/3}, \tag{4}$$

which we will refer to as the acceleration limit. To achieve this limit, we must have $v_x<\hbar/(2M\Delta x_{\rm accel})$, as shown below. For a 10^{12}-Hz/cm light-shift gradient, the optimum resolution is about 70 Å for samarium and the required collimation for a beam of speed 6×10^4 cm/s is 50 μrad, which is not too stringent.

(3) *Uncertainty limit.* Since the force due to the spatially varying potential acts on the atom only after it makes a transition from the initial unshifted state, the momentum uncertainty imparted by the force, Δp, is approximately equal to the maximum momentum imparted, FT. Using Eq. (2) we see that the final state is created with a spatial resolution and momentum spread which obey the uncertainty relation $\Delta x\Delta p\simeq\hbar$. In Sec. III B it is shown that *minimum* uncertainty packets can be created under appropriate conditions.

(4) *Detection.* The method for detecting the final state (f) need not have any spatial resolution since the measurement is done by the Raman region. Only the spatial integral of the final-state flux is needed, therefore a variety of final-state detection schemes are possible. These include resonance fluorescence, and single-atom methods such as photon burst and photoionization, which have been successfully applied to trace-element measurement.

II. THEORY

In the following, we consider the Raman-induced resonance imaging scheme[7] in detail. Schemes based on one-photon transitions, when appropriate, yield analagous results and need not be derived in depth. A three-level atom with states i,I,f, as shown in Fig. 2, enters a region with a spatially varying potential which exerts a force on the state f only. The atom enters the region in state i which does *not* interact with the spatially varying potential and makes a Raman transition via two off-resonant light fields to the final state. The transition occurs in a localized region determined by the resonance condition that the initial- to-final-state frequency ω_{fi} equal the difference frequency of the two applied optical fields. The total (spatially integrated) final-state flux emerging from the Raman region is monitored downstream as a function of the Raman-field difference frequency or as a function of ω_{fi} which can be tuned by means of an applied uniform magnetic field.

In this section, the integrated flux of atoms in state f exiting the Raman region is calculated at distances large compared to the diameter of the Raman regions which are assumed to be Gaussian. The steady-state amplitude for the final state is calculated first, where it is assumed that the wave-mechanical motion is important for the x motion. An eikonal approximation is assumed to be adequate for the y coordinate along the atomic-beam axis. The Raman transition frequency ω_{fi} is taken to be very small, so that the difference in the wave vectors of the optical fields can be taken as zero. In this case, the net recoil momentum of the atom in making the Raman transition is negligible. Finally, the optical fields are assumed to be far enough off resonance with the excited state that the excited-state amplitude can be adiabatically eliminated from the coupled amplitude equations which are derived below.

The Hamiltonian for the three-level system of Fig. 2 is

taken as

$$H=\frac{\mathbf{P}^2}{2M}+H^{(0)}-\boldsymbol{\mu}\cdot\mathbf{E}(\mathbf{R},t)-(x-x_0)F^{\mathrm{op}}\ , \tag{5}$$

where $H^{(0)}$ is the internal Hamiltonian, $\mathbf{P}$ is the atomic center-of-mass momentum operator, F^{op} is the external force operator, and x is the position along the measurement axis. The electric dipole operator is $\boldsymbol{\mu}$ and the applied field is of the form

$$\mathbf{E}(\mathbf{R},t)=\left[\frac{\hat{\mathbf{e}}_1\mathcal{E}_1}{2}e^{i(\mathbf{q}\cdot\mathbf{R}-\Omega_1 t)}+\text{c.c.}+\frac{\hat{\mathbf{e}}_2\mathcal{E}_2}{2}e^{i(\mathbf{q}\cdot\mathbf{R}-\Omega_2 t)}+\text{c.c.}\right]e^{-1/2[(y-y_1)/d)]^2}\ , \tag{6}$$

where the Raman fields are assumed to copropagate and the difference frequency $\Omega_1-\Omega_2$ is assumed sufficiently small that the wave vectors are taken to be of equal magnitude. The polarizations $\hat{\mathbf{e}}_{1,2}$ are chosen so that each field interacts with only one transition. The Raman-field region is taken to be centered at a position y_1 along the atomic-beam axis and the laser $1/e$ intensity radius along the y axis is d. Variation in the fields along directions perpendicular to the atomic-beam axis is assumed negligible. The atomic wave function is taken to be of the form

$$|\Psi(\mathbf{R},t)\rangle=\sum_n\frac{e^{i\mathbf{k}\cdot\mathbf{R}}}{\sqrt{V}}e^{-i(\hbar\mathbf{k}^2/2M)t}A_n(\mathbf{R},t)e^{-i\omega_n t}|n\rangle\ , \tag{7}$$

where the velocity of the particular atom being considered is $\mathbf{v}=\hbar\mathbf{k}/M$ prior to interaction and it is assumed that an initial velocity average will be performed at the end of the calculation. The internal state of energy $\hbar\omega_n$ is $|n\rangle$. With these assumptions, the time-dependent Schrödinger equation yields equations of motion for the state amplitudes A_n given by

$$i\hbar\left[\frac{\partial}{\partial t}+\mathbf{v}\cdot\nabla\right]A_n+\frac{\hbar^2}{2M}\nabla^2A_n+(x-x_0)F_nA_n=-\sum_m\boldsymbol{\mu}_{nm}\cdot\mathbf{E}(\mathbf{R},t)e^{i\omega_{nm}t}A_m\ , \tag{8}$$

where the force $F_n=F\delta_{nf}$ acts only on the final state. We take the Raman difference frequency equal to the $i\rightarrow f$ frequency in the absence of the force: $\Omega_1-\Omega_2=\omega_{fi}$. Then we seek solutions for which the initial- and final-state amplitudes are time independent but vary in space. It is assumed that the velocity perpendicular to the laser beams v_y is large (i.e., a thermal speed), while the velocity v_x along the measurement axis x is small. In this case, it is convenient to make an eikonal approximation for the y motion, retaining only the first spatial derivative term, while for the x direction, both the first and second x derivatives are retained to take into account packet spreading. Equation (8) is then easily solved in perturbation theory by finding the Green's function for states i and f and treating the right-hand side as a source.

To proceed, Eq. (8) is rewritten explicitly using the rotating-wave approximation and takes the form

$$\begin{aligned}
&\left[\frac{\partial}{\partial t}+\mathbf{v}\cdot\nabla-\frac{i\hbar}{2M}\frac{\partial^2}{\partial x^2}\right]A_i(\mathbf{R},t)=-\frac{\Omega_{Ii}^*(\mathbf{R})}{2i}e^{-i\mathbf{q}\cdot\mathbf{R}-i(\omega_{Ii}-\Omega_1)t}A_I(\mathbf{R},t)\ ,\\
&\left[\frac{\partial}{\partial t}+\mathbf{v}\cdot\nabla-\frac{i\hbar}{2M}\frac{\partial^2}{\partial x^2}-\frac{i}{\hbar}(x-x_0)F\right]A_f(\mathbf{R},t)=-\frac{\Omega_{If}^*(\mathbf{R})}{2i}e^{-i\mathbf{q}\cdot\mathbf{R}-i(\omega_{If}-\Omega_2)t}A_I(\mathbf{R},t)\ ,\\
&\left[\frac{\partial}{\partial t}+\mathbf{v}\cdot\nabla-\frac{i\hbar}{2M}\frac{\partial^2}{\partial x^2}\right]A_I(\mathbf{R},t)=-\frac{\Omega_{Ii}(\mathbf{R})}{2i}e^{+i\mathbf{q}\cdot\mathbf{R}+i(\omega_{Ii}-\Omega_1)t}A_i(\mathbf{R},t)\\
&\qquad-\frac{\Omega_{If}(\mathbf{R})}{2i}e^{+i\mathbf{q}\cdot\mathbf{R}+i(\omega_{If}-\Omega_2)t}A_f(\mathbf{R},t)-\frac{\gamma_s}{2}A_I(\mathbf{R},t)\ ,
\end{aligned} \tag{9}$$

where $\Omega_{Ii}(\mathbf{R})=\boldsymbol{\mu}_{Ii}\cdot\hat{\mathbf{e}}_1\mathcal{E}_1(\mathbf{R})/\hbar$ and $\Omega_{If}(\mathbf{R})=\boldsymbol{\mu}_{If}\cdot\hat{\mathbf{e}}_2\mathcal{E}_2(\mathbf{R})/\hbar$ and the spatial dependence of the fields is given by the Gaussian distribution of Eq. (6). The convective derivative term describes a straight-line trajectory for constant velocity, the second derivative term in x allows for diffraction (wave-packet spreading), and the force term takes into account the spatially varying potential which affects only the final state.

It is assumed that the Raman fields are detuned far from resonance with the intermediate state so that coherent transitions from the initial state to the final state are dominant over incoherent optical pumping. In this case, the intermediate-state amplitude A_I can be adiabatically eliminated from Eqs. (9). Suppose that $\Omega_1-\Omega_2=\omega_{fi}=\omega_{Ii}-\omega_{If}$ so that $\omega_{Ii}-\Omega_1=\omega_{If}-\Omega_2\equiv-\Delta$. In the large-detuning limit, we have $\Delta\gg\gamma_s$, $\mathbf{q}\cdot\mathbf{v}$, Ω_{Ii}, Ω_{If}, etc. Letting $A_I(t)=a_I(t)\exp(-i\Delta t)$ in Eqs. (9), the intermediate-state amplitude is approximately given by

$$A_I(t)\simeq-\frac{\Omega_{Ii}(\mathbf{R})}{2i\left[\frac{\gamma_s}{2}-i\Delta\right]}e^{i\mathbf{q}\cdot\mathbf{R}-i\Delta t}A_i(\mathbf{R},t)-\frac{\Omega_{If}(\mathbf{R})}{2i\left[\frac{\gamma_s}{2}-i\Delta\right]}e^{i\mathbf{q}\cdot\mathbf{R}-i\Delta t}A_f(\mathbf{R},t)\ . \tag{10}$$

With Eq. (10), the evolution equations (9) for the initial- and final-state amplitudes take the form

$$\left[\frac{\partial}{\partial t}+\mathbf{v}\cdot\nabla-\frac{i\hbar}{2M}\frac{\partial^2}{\partial x^2}\right]A_i(\mathbf{R},t)$$
$$=-\frac{|\Omega_{Ii}(\mathbf{R})|^2}{4(\gamma_s/2-i\Delta)}A_i-\frac{\Omega_{Ii}^*(\mathbf{R})\Omega_{If}(\mathbf{R})}{4\left[\frac{\gamma_s}{2}-i\Delta\right]}A_f\ ,$$
$$\left[\frac{\partial}{\partial t}+\mathbf{v}\cdot\nabla-\frac{i\hbar}{2m}\frac{\partial^2}{\partial x^2}-\frac{i}{\hbar}(x-x_0)F\right]A_f(\mathbf{R},t)$$
$$=-\frac{|\Omega_{If}(\mathbf{R})|^2}{4\left[\frac{\gamma_s}{2}-i\Delta\right]}A_f-\frac{\Omega_{Ii}(\mathbf{R})\Omega_{If}^*(\mathbf{R})}{4\left[\frac{\gamma_s}{2}-i\Delta\right]}A_i\ . \tag{11}$$

Equations (11) are readily solved in perturbation theory. This yields a spatial resolution function (see below) which includes the effects of both classical motion and diffraction of the moving atoms. In lowest order, the initial-state amplitude $A_i^{(0)}(y,x)$ can be taken to propagate neglecting the Raman fields. Further, the velocity will be taken to have only x and y components. It is assumed that the atomic distribution does not vary in the z direction. Then, the initial-state amplitude satisfies

$$\left[v_y\frac{\partial}{\partial y}+v_x\frac{\partial}{\partial x}-\frac{i\hbar}{2M}\frac{\partial^2}{\partial x^2}\right]A_i^{(0)}(y,x)=0\ . \tag{12}$$

The solution to this equation is determined by free-particle propagation, where y/v_y plays the role of the time. If the amplitude A_i is specified in the plane located at y_1 along the atomic-beam axis, then the amplitude at an arbitrary position y_2',x_2' is evidently given by

$$A_i^{(0)}(y_2',x_2')=\int_{-\infty}^{\infty}dx_1'A_i(y_1,x_1')\int dk_1\frac{1}{2\pi}e^{ik_1[x_2'-x_1'-v_x(y_2'-y_1)/v_y]}e^{-i(\hbar k_1^2/2m)(y_2'-y_1)/v_y}\ . \tag{13}$$

To lowest order in the Raman fields, the term on the right-hand side of the A_f evolution equation (11) proportional to A_f may be neglected, since A_f is assumed to be initially zero, prior to a Raman transition from state i. (That is, we neglect the light shift and optical pumping due to the weak nonresonant Raman fields. In practice, the Raman-field intensities are adjusted to give equal light shifts which cancel for the $i\rightarrow f$ transition.) The solution for the final-state amplitude in the y,x plane is then readily obtained by means of the Green's function which satisfies

$$\left[v_y\frac{\partial}{\partial y}+v_x\frac{\partial}{\partial x}-\frac{i\hbar}{2M}\frac{\partial^2}{\partial x^2}-i(x-x_0)\frac{F}{\hbar}\right]G_F(y,y_2';x,x_2')=\delta(y-y_2')\delta(x-x_2')\ . \tag{14}$$

The final-state amplitude is given by

$$A_f(y,x)=\int dy_2'\int dx_2'G_F(y,y_2';x,x_2')\frac{-\Omega_{Ii}(y_2')\Omega_{If}^*(y_2')}{4\left[\frac{\gamma_s}{2}-i\Delta\right]}A_i^{(0)}(y_2',x_2')\ , \tag{15}$$

where the Rabi frequencies are taken to be Gaussian distributions centered at y_1 along the y axis [see Eq. (6)] but independent of x for simplicity (i.e., the measurement length is taken to be small compared to the radius and the Rayleigh length of the Raman beams).

As shown in Appendix A, the required Green's function for propagating in a uniform force field is obtainable by transforming to momentum space and is given by

$$G_F(y,y_2';x,x_2')=\frac{\Theta(y-y_2')}{v_y}\int_{-\infty}^{\infty}dk\frac{1}{2\pi}\exp\left\{ik\left[x-x_2'-v_x\frac{y-y_2'}{v_y}-\frac{F}{2M}\left[\frac{y-y_2'}{v_y}\right]^2\right]\right\}e^{-i[(\hbar k^2/2M)][(y-y_2')/(v_y)]}$$
$$\times\exp\left[i\frac{F}{\hbar}\frac{y-y_2'}{v_y}(x-x_0)-i\frac{Fv_x}{2\hbar}\left[\frac{y-y_2'}{v_y}\right]^2-i\frac{F^2}{6\hbar M}\left[\frac{y-y_2'}{v_y}\right]^3\right]\ . \tag{16}$$

In this form, the Green's function has a simple physical interpretation. Neglecting wave-packet spreading, integration over k for the first exponential factor yields a δ function requiring the atom to follow the classical trajectory during the time $(y-y_2')/v_y$. The second exponential takes wave-packet spreading into account. The last exponential factor is just the phase acquired by the final state of the atom in propagating through the classical path in the potential due to the force field.

In Appendix B, the integrated final-state flux emerging from the Raman region is evaluated starting from Eq. (15) and yields the following result:

$$\int_{-\infty}^{\infty} dx\,|A_f(y,x)|^2 = \left|\frac{\Omega_{Ii}\Omega_{If}^*}{4v_y\left[\frac{\gamma_s}{2}-i\Delta\right]}\right|^2 \int dx_1' \int_{-\infty}^{\infty} du_- \int_{-\infty}^{\infty} du_+ e^{-(u_-^2/2d^2)} e^{-(2u_+^2/d^2)} \times e^{-i[(Fv_x)/(\hbar v_y^2)]u_+u_-} e^{-i[(F)/(\hbar v_y)](x_1'-x_0)u_- - i[(F^2)/12\hbar M v_y^3)]u_-^3} \times A_i\left[y_1, x_1' - \frac{F}{2Mv_y^2}u_+u_-\right] A_i^*\left[y_1, x_1' + \frac{F}{2Mv_y^2}u_+u_-\right]. \quad (17)$$

Equation (17) gives the general result for the integrated flux in the final state in terms of an arbitrary initial-state amplitude specified at the center of the Raman region $y=y_1$, $A_i(y_1,x)$. To obtain the final-state count rate, this result must be multiplied by the atomic density, the atomic-beam velocity, and the transverse dimension of the atomic beam perpendicular to the measurement axis.

III. RESULTS

In the following sections, the spatial resolution obtained with the Raman-induced resonance imaging method is examined first, in order to verify the statements made in the Introduction based on heuristic arguments. Then, the final-state wave function is examined to determine the momentum and position distribution of the final-state atoms. For a plane-wave input in the initial state, it is shown that under appropriate circumstances, a minimum-uncertainty final-state wave packet may be obtained.

A. The spatial resolution function

Using the result given by Eq. (17), the spatially integrated final-state flux can be determined for any given spatially varying initial-state amplitude $A_i(y_1,x)$. This determines the dependence of the signal on the applied uniform magnetic field (i.e., on the resonant point x_0). Further, in an important special case, described below, this result is to determine the general form of the sampling function which measures the incident atomic distribution in state i. We will refer to this sampling function as the resolution function.

The Gaussian factors in the integrand of Eq. (17) constrain $u_\pm$ to distances of order d. If the initial-state amplitude does not vary over distances of order $(F/2M)(d/v_y)^2$, then the dependence of the amplitudes on $u_\pm$ may be neglected. This requires that the interaction time d/v_y in the Raman fields be not too large, so that the final state does not accelerate over distances comparable to the length scale over which the initial-state amplitude varies. In this case, the u_+ integration is readily done and the integrated flux then takes the form

$$\int_{-\infty}^{\infty} dx\,|A_f(y,x)|^2 = \left|\frac{\Omega_{Ii}\Omega_{If}^* d\sqrt{\pi}}{\left[\frac{\gamma_s}{2}-i\Delta\right]4v_y}\right|^2 \times \int dx_1' R_1(x_1'-x_0) \times |A_i(y_1,x_1')|^2, \quad (18)$$

where the resolution function R_1 is given by

$$R_1(x_1'-x_0) = \int_{-\infty}^{\infty} du_- \frac{1}{(2\pi d^2)^{1/2}} \exp\left\{-\left[\frac{1}{2d^2}+\frac{1}{8}\left[\frac{Fv_x d}{\hbar v_y^2}\right]^2\right]u_-^2\right\} \exp\left[-i\frac{F}{\hbar v_y}(x_1'-x_0)u_- - i\frac{F^2}{12\hbar M v_y^3}u_-^3\right]. \quad (19)$$

Physically, the meaning of this result is clear. The exponent in the Gaussian factor decreases as the Raman beam radius d is made larger and the interaction time longer, corresponding to higher-frequency resolution. This tends to increase the spatial resolution and narrow the resolution function. However, as d is increased, the motion along the measurement axis due to v_x tends to increase the exponent and broadens the resolution function. The acceleration of the final state leads to a phase factor in the integrand which is cubic in the time (u_-/v_y), as one would expect using classical arguments. In addition, diffraction also leads to a cubic time dependence of the phase.

This result can be cast in a simpler form by using the natural length scales for this problem which are discussed in the Introduction. The form of the resulting resolution function serves to justify the heuristic treatment of the resolution limits.

It is convenient to express distance along the measurement axis in units of the acceleration limited-resolution length, Eq. (4). The resolution length in turn leads to the natural unit of transit time across the Raman

region, T_0. Using $(F/2M)T_0^2=\Delta x_{\text{accel}}$ one obtains $T_0=(2M\hbar/F^2)^{1/3}$. The corresponding unit of distance along the atomic-beam axis, y, is just $d_0=v_y T_0$. Defining $u_-=\eta d_0$, and expressing $x_1'-x_0$ in units of Δx_{accel}, the resolution function can be recast into the following form:

$$R_0(x_1'-x_0)=\frac{1}{\Delta x_{\text{accel}}} I\left[\frac{x_1'-x_0}{\Delta x_{\text{accel}}}\right], \tag{20}$$

where

$$I(s)=\int_{-\infty}^{\infty} d\eta \frac{1}{2\pi} e^{-\alpha(\eta^2/2)} e^{-i\,\text{sgn}(F)s\eta - i(\eta^3/6)}$$
$$=\int_0^{\infty} d\eta \frac{1}{\pi} e^{-\alpha(\eta^2/2)} \cos\left[\text{sgn}(F)s\eta+\frac{\eta^3}{6}\right], \tag{21}$$

with $\text{sgn}(F)=+1(-1)$ for a positive (negative) force. Note that $\int dx_1' R_0(x_1'-x_0)=1$. The parameters appearing in Eq. (21) are given by

$$\alpha=\frac{d_0^2}{d^2}+\frac{d^2}{d_0^2}r^4,$$
$$r=\frac{\Delta x_{\text{vel}}}{2\Delta x_{\text{accel}}},$$
$$\Delta x_{\text{vel}}=\left[\frac{2\hbar v_x}{|F|}\right]^{1/2}, \tag{22}$$
$$d_0=v_y\left[\frac{2M\hbar}{F^2}\right]^{1/3}.$$

In terms of R_0, the integrated final-state flux takes the form

$$\int_{-\infty}^{\infty} dx\,|A_f(y,x)|^2$$
$$=\eta_R\frac{\sqrt{2\pi}\hbar v_y}{d|F|}\int dx'\,|A_i(y_1,x')|^2 R_0(x'-x_0)$$
$$\simeq\eta_R\frac{\sqrt{2\pi}\hbar v_y}{d|F|}|A_i(y_1,x'=x_0)|^2, \tag{23}$$

where the approximate result is valid if the resolution function is narrow compared to the length scales over which the atomic distribution varies. The Raman transition probability is given by

$$\eta_R=\left|\frac{\Omega_{Ii}\Omega_{If}^* d\sqrt{\pi}}{\left[\frac{\gamma_s}{2}-i\Delta\right]4v_y}\right|^2. \tag{24}$$

Note that the factor which multiplies the Raman transition probability in Eq. (23) is of the order of the position resolution. The approximate result could, of course, have been written down on the basis of physical arguments, without detailed calculation. The important feature is that the detailed shape of the resolution function is obtained.

According to Eqs. (20) and (21), the resolution function will be approximately Gaussian if the parameter α is large compared to unity, so that the cubic dependence of the phase on η can be neglected. When the velocity is so large that $\Delta x_{\text{vel}}>\Delta x_{\text{accel}}$, which implies $v_x>\hbar/2M\Delta x_{\text{accel}}$, the factor r^4 in α of Eq. (22) quickly becomes large and Gaussian dependence dominates the integrand. In this limit, the resolution function takes the form

$$I(s)=\frac{e^{-s^2/2\alpha}}{\sqrt{2\pi\alpha}}. \tag{25}$$

According to Eq. (22), the parameter α is minimized for a certain value of the Raman-region diameter d. Physically, the frequency resolution increases as d is increased. This tends to increase the position resolution. However, the velocity along the measurement axis v_x causes the position to move during the measurement. Hence, an optimum diameter exists. Differentiating α with respect to d, and setting the result equal to zero, one obtains $d_{\text{opt}}=d_0/r$ and $\alpha_{\text{opt}}=2r^2$. The corresponding resolution function then is given by Eqs. (20) and (25) as

$$R_0(x_1'-x_0)=\frac{\exp\left[-\left[\frac{x_1'-x_0}{\Delta x_{\text{vel}}}\right]^2\right]}{\Delta x_{\text{vel}}\sqrt{\pi}} \tag{26}$$

and $d_{\text{opt}}=(v_y/v_x)\Delta x_{\text{vel}}$. Physically, the atom travels a distance along the measurement axis just equal to the optimum resolution length during the transit time across the Raman region. Note that the neglect of $Fu_+u_-/2Mv_y^2$ in the argument of the initial amplitude A_i in Eq. (17) is justified if A_i varies slowly compared to $Fd_{\text{opt}}^2/2Mv_y^2=\hbar/2Mv_x<\Delta x_{\text{accel}}$ in this limit.

In the opposite limit when $\Delta x_{\text{vel}}<\Delta x_{\text{accel}}$, i.e., when $v_x<\hbar/2M\Delta x_{\text{accel}}$, the ratio r is less than unity and the parameter $\alpha\simeq d_0^2/d^2$. Hence, as the Raman-region diameter d is increased to order d_0 or greater, α decreases, and the functions $I(s)$ and R_0 narrow. As $\alpha\to 0$, it is clear from the exact equation (21) for $I(s)$ that the natural length scale for s is unity, since the cubic phase plays the dominant role in the integrand. This corresponds to spatial resolution comparable to the acceleration length. The function $I(s)$ is plotted in Fig. 3 for various values of α.

When α is of order unity (1–2), the shape is nicely localized and is nearly Gaussian. However, if α is made small, corresponding to a large Raman-region diameter, the function $I(s)$ is asymmetric. It oscillates on one side and decays on the other. Physically, this is linked to the fact that for a positive force, the final-state amplitude created at x' to the left of the resonance position x_0 within a distance of order Δx_{accel} accelerates to the right and interferes with the amplitude created at x_0. Hence, the resolution function oscillates on the left side of x_0 for a positive force. However, final-state amplitude created

for x' to the right of x_0 accelerates further to the right away from x_0 and hence does not interfere. Thus, the resolution function rapidly dies off on this side of x_0 for a positive force. This behavior is, of course, related to the wave function for penetration of a potential barrier which varies linearly in position, but is opposite to what one might expect because the final state is accelerated rather than the initial state.

B. Minimum-uncertainty spatial wave packets

The process of measuring the initial-state distribution via the Raman-induced resonance imaging method naturally creates the final-state spatial wave function in the form of a localized packet, since the $i \rightarrow f$ transition occurs in a highly localized spatial region. Hence, the method is well suited to the creation and study of spatial wave packets and it is of interest to determine the momentum and position spread of such a state. For this purpose, we assume for simplicity that the initial state takes the form of a plane wave with $A_i(y_1,x)=1$. In this case, the final-state spatial wave function after the Raman region where $y > y_1$ can be evaluated starting from Eq. (B6). The x_1' integration is straightforward and yields the unnormalized state for an atom of initial velocity $\mathbf{v}=\hbar\mathbf{k}/M$ as $\psi_f(y,x)=e^{i\mathbf{k}\cdot\mathbf{R}}A_f(y,x)$. Choosing a normalization constant so that $\int_{-\infty}^{\infty}dx\,|\psi_f(y,x)|^2=1$ yields the final-state wave function in the form

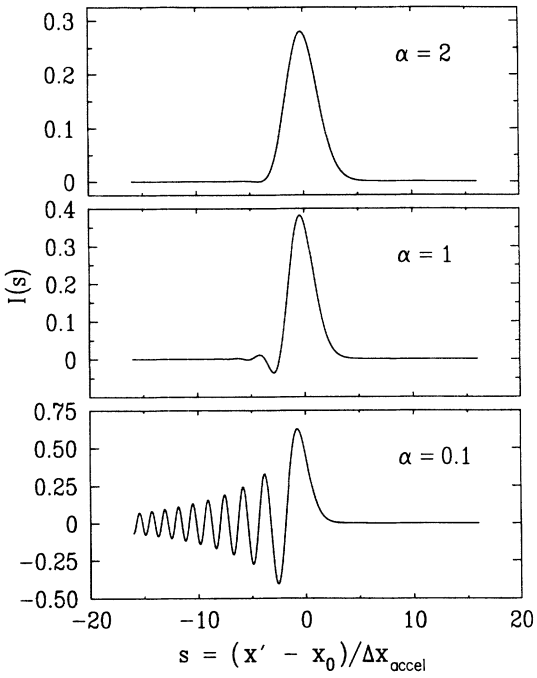

FIG. 3. Spatial resolution function. The s axis denotes position along the measurement axis in units of the optimum acceleration limited resolution length (see text).

$$\psi_f(y,x)=\left[\frac{2\pi d^2\hbar v_y}{|F|d}\left[\frac{\pi}{2}\right]^{1/2}\right]^{-1/2}e^{i\mathbf{k}\cdot\mathbf{R}}$$
$$\times\int_{-\infty}^{\infty}dy_2'\exp\left[-\left[\frac{y_2'-y_1}{d}\right]^2\right]\exp\left\{i\left[\frac{F}{\hbar}\frac{y-y_2'}{v_y}(x-x_0)-\frac{Fv_x}{2\hbar}\left[\frac{y-y_2'}{v_y}\right]^2-\frac{F^2}{6\hbar M}\left[\frac{y-y_2'}{v_y}\right]^3\right]\right\}. \quad (27)$$

Using Eq. (27), the momentum spread of the final-state wave packet is readily evaluated, since differentiation with respect to x just differentiates the phase factors and evaluation of the expectation values then requires only Gaussian integrals. The momentum spread is found to be

$$(\Delta p)^2\equiv\overline{p^2}-\bar{p}^2=M^2(\Delta v_x)^2+\left[\frac{Fd}{2v_y}\right]^2, \quad (28)$$

where the first term arises from a thermal average over the transverse velocity spread and the spread in the longitudinal velocity v_y along the atomic beam is ignored for simplicity. For a supersonic atomic beam, this is a reasonable approximation. With adequate beam collimation, the acceleration limit is attained and yields $(\Delta p)^2=[(Fd)/2v_y)]^2$.

The position spread also can be evaluated from Eq. (27) using integration by parts and the identity

$$\int_{-\infty}^{\infty}du\,u^n\exp i\left[\frac{F}{\hbar}\frac{y_1'-y_2'}{v_y}u\right]$$
$$=\frac{2\pi}{|F/\hbar v_y|}\left[\frac{-\hbar v_y}{iF}\frac{\partial}{\partial y_2'}\right]^n\delta(y_2'-y_1'). \quad (29)$$

This yields

$$(\Delta x)^2\equiv\overline{x^2}-\bar{x}^2=\left[\frac{\hbar v_y}{Fd}\right]^2+\left[\frac{Fd^2}{2Mv_y^2}\right]^2\left[\frac{3}{16}+\left[\frac{y-y_1}{d}\right]^2\right]+(\Delta v_x)^2\left[\frac{y-y_1}{v_y}\right]^2+\frac{F\overline{v_x}}{Mv_y^3}\frac{d^2(y-y_1)}{4}+\overline{v_x^2}\frac{d^2}{4v_y^2}, \quad (30)$$

where the overline on the v_x terms indicates a thermal average over the initial transverse velocity spread and the v_y spread is again ignored. For these equations to be valid, the observation point must be after the Raman region, so that $y-y_1$ must be somewhat greater than d.

Using the position and momentum spread, the uncertainty product can be obtained. The most interesting case is that of high collimation where the spread in v_x

satisfies $\Delta v_x < \hbar/(M\Delta x_{\text{accel}})$ and the acceleration limit is achieved. In this case, the transverse coherence length of the incident beam is greater than Δx_{accel} and the force F imparts a momentum larger than the transverse thermal spread. Neglecting the transverse velocity spread terms, the uncertainty product then takes the form

$$(\Delta x)^2(\Delta p)^2=\frac{\hbar^2}{4}\left\{1+\left[\frac{d}{d_0}\right]^6\left[\frac{3}{16}+\left[\frac{y-y_1}{d}\right]^2\right]\right\}, \tag{31}$$

where d_0 is the natural unit of distance along the atomic-beam axis in the acceleration limit, Eq. (22). For observation points not too far after the Raman region, $y-y_1$ is of the order of Raman region size d and Eq. (31) shows that a minimum uncertainty state is rapidly approached as the radius d is reduced somewhat below d_0. Physically, this is easy to understand. When the radius d of the Raman region is reduced below the size d_0 which achieves optimum position resolution in the acceleration limit, atomic acceleration and diffraction during the transit time across the Raman region are negligible. In this case, the atom in its rest frame sees a Gaussian frequency pulse without chirping. Due to the linear spatial variation of the final-state potential, the Gaussian frequency distribution selects out a Gaussian spatial distribution for the final-state wave packet. This follows from Eq. (27) when the quadratic terms in the phase due to v_x and cubic terms due to the acceleration are neglected, which leads to a Gaussian spatial wave function for the final state.

IV. CONCLUSIONS

The calculation of the form of the resolution function and of the final-state wave function above justifies the statements made in Ref. 7 on the basis of heuristic arguments. The results for the ultimate spatial resolution Δx_{accel} show that very high spatial resolution is attainable for large spatially varying final-state level shifts. For example, a samarium atomic beam of nominal speed 6×10^4 cm/s in a level shift gradient of 10^{12} Hz/cm yields a spatial resolution $\simeq 70$ Å. To obtain this resolution, it is necessary that $\Delta x_{\text{vel}} < \Delta x_{\text{accel}}$ which is equivalent to $v_x < \hbar/(2M\Delta x_{\text{accel}})$. For the above conditions, this requires $v_x < 3$ cm/s corresponding to a beam collimation better than 50 μm. The optimum Raman beam intensity $1/e$ radius d is about 140 μm in this case. Note that the Doppler shifts due to divergence of the Raman beams cancel if the beam radii are matched at the focus.

For large spatially varying level shift gradients, the frequency resolution required to obtain the optimum spatial resolution is not as stringent as for small gradients. In this case, a simple one-photon transition may be applicable with long-lived excited states to achieve very high spatial resolution. For example, in ^{174}Yb, this method can be applied to excite the $^1S_0\rightarrow{}^3P_1$ transition and either absorption or resonance fluorescence in the interaction region can be directly measured by modulating the level shift gradient as done by Salomon *et al.*[3] In this case, for suboptical wavelength spatial resolution the recoil momentum for a one-photon process will be negligible compared to the momentum imparted by the spatially varying potential.

An important application of the Raman-induced resonance imaging method is in the development of *two-point* correlation techniques. By employing two pairs of Raman difference frequencies, it is possible to access two separated spatial points with high spatial resolution. The final states for each of the regions can be made either identical or different so that the contribution of each region to the total detected signal can be made either distinguishable or indistinguishable. The use of two-point correlation measurements opens up the possibility of achieving the atomic analogue of the optical intensity correlations originally explored by Brown and Twiss. In this type of technique, only the transverse coherence length needs to be longer than the spatial separation between detection regions. This type of detection can be applied to perform atom antibunching experiments and is likely to be of use in studying atomic spatial coherence.

The simplicity of the proposed optical measurement methods suggests that experiments based on these techniques may be useful in studying quantum-mechanical features of atomic-position measurement in general.[11] Interesting applications include the creation and study of one-dimensional wave packets, which, as shown above, can be minimum-uncertainty Gaussian states under appropriate conditions. The evolution of position-squeezed states[12] also may be observable with one-dimensional harmonic wells based on spatially varying light-shift potentials.

ACKNOWLEDGMENTS

The author is indebted to George Welch and Jeff Gardner for many stimulating discussions and for carefully reading and commenting on the manuscript. This research is supported by Rome Air Development Center through Contract No. F19628-88-K-0012.

APPENDIX A. DERIVATION OF THE GREEN'S FUNCTION FOR PROPAGATION IN A UNIFORM FORCE FIELD

According to Eq. (14) of the text, the required Green's function satisfies

$$\left[v_y\frac{\partial}{\partial y}+v_x\frac{\partial}{\partial x}-\frac{i\hbar}{2M}\frac{\partial^2}{\partial x^2}-i(x-x_0)\frac{F}{\hbar}+\epsilon\right]G_F(y,y_2';x,x_2')=\delta(y-y_2')\delta(x-x_2'), \tag{A1}$$

where a positive infinitesimal (ϵ) is added to the equation to ensure causality. The Green's function can be found by

Fourier-transform techniques. We begin by assuming the form

$$G(y,y';x,x')=\int\int dk_y dk_x \frac{1}{(2\pi)^2} G(k_y,k_x) e^{i(k_y y+k_x x)} . \tag{A2}$$

Substituting Eq. (A2) into Eq. (A1) yields

$$\int\int dk_y dk_x \frac{1}{(2\pi)^2}\left[ik_y v_y+ik_x v_x+\frac{i\hbar}{2M}k_x^2+i\frac{F}{\hbar}x_0+\epsilon\right] G(k_y,k_x)e^{i(k_y y+k_x x)}$$
$$-\frac{F}{\hbar}\int\int dk_y dk_x \frac{1}{(2\pi)^2}\left[\frac{\partial}{\partial k_x}e^{i(k_y y+k_x x)}\right] G(k_y,k_x)=\int\int dk_y dk_x \frac{1}{(2\pi)^2} e^{ik_y(y-y')+ik_x(x-x')} . \tag{A3}$$

The integral involving the derivative of the exponential, which arises from the x-dependent term in Eq. (A1), can be integrated by parts assuming $G(k_y,k_x=\pm\infty)=0$. The surface terms then vanish, and the Fourier transform is found to satisfy

$$\frac{F}{\hbar}\frac{\partial G(k_y,k_x)}{\partial k_x}+i\left[k_y v_y+k_x v_x+\frac{\hbar}{2M}k_x^2+\frac{F}{\hbar}x_0-i\epsilon\right] G(k_y,k_x)=e^{-i(k_y y'+k_x x')} . \tag{A4}$$

Note that the same equation is obtained by Fourier transforming Eq. (A1) with $\int\int dy\,dx \exp -i(k_y y+k_x x)$, provided that $G(y\to\pm\infty, x\to\pm\infty)\to 0$. This equation is readily solved using an integrating factor. Let (for $F\neq 0$)

$$G(k_y,k_x)=A(k_y,k_x)\exp\left[-i\frac{\hbar}{F}\int_a^{k_x}\left[k_y v_y+k_x' v_x+\frac{\hbar k_x'^2}{2M}+\frac{F}{\hbar}x_0-i\epsilon\right]dk_x'\right] , \tag{A5}$$

where a is an undetermined constant. Then,

$$\frac{F}{\hbar}\frac{\partial A(k_y,k_x)}{\partial k_x}=\exp\left[i\frac{\hbar}{F}\int_a^{k_x}\left[k_y v_y+k_x' v_x+\frac{\hbar k_x'^2}{2M}+\frac{F}{\hbar}x_0-i\epsilon\right]dk_x'\right] e^{-ik_y y'-ik_x x'} . \tag{A6}$$

This has the solution

$$A(k_y,k_x)=\frac{\hbar}{F}\int_b^{k_x} dk_x'' \exp\left[i\frac{\hbar}{F}\int_a^{k_x''}\left[k_y v_y+k_x' v_x+\frac{\hbar k_x'^2}{2M}+\frac{F}{\hbar}x_0-i\epsilon\right]dk_x'\right] e^{-ik_y y'-ik_x'' x'} . \tag{A7}$$

Then

$$G(k_y,k_x)=\frac{\hbar}{F}\int_b^{k_x} dk_x'' e^{-ik_y y'-ik_x'' x'} \exp\left[-i\frac{\hbar}{F}\int_{k_x''}^{k_x}\left[k_y v_y+k_x' v_x+\frac{\hbar k_x'^2}{2M}+\frac{F}{\hbar}x_0-i\epsilon\right]dk_x'\right] , \tag{A8}$$

where the constant a in Eq. (A5) drops out. As $k_x\to\infty$, $G(k_y,k_x)\to 0$ for positive F, since $\exp(-(\epsilon\hbar/F)\int_{k_x''}^{k_x})\to 0$. To ensure that $G(k_x\to-\infty)\to 0$, we must take $b=-\infty$. However, if $F<0$, we need $b=+\infty$, so that $k_x''>k_x$. Then, again as $k_x\to\pm\infty$, $G(k_y,k_x)\to 0$.

With Eqs. (A8) and (A2), the Green's function then takes the form

$$G(y,y';x,x')=\int\int dk_y dk_x \frac{1}{(2\pi)^2} e^{ik_y(y-y')+ik_x x}\frac{\hbar}{F}\int_b^{k_x} dk_x'' e^{-ik_x'' x'} \exp\left[-i\frac{\hbar}{F}\int_{k_x''}^{k_x}\left[k_y v_y+k_x' v_x+\frac{\hbar k_x'^2}{2M}+\frac{F}{\hbar}x_0\right]dk_x'\right] . \tag{A9}$$

To incorporate the boundary conditions in an F-independent manner, it is convenient to change variables, letting $k_x=(F/\hbar)\tau$, $k_x'=(F/\hbar)\tau'$, and $k_x''=(F/\hbar)\tau''$. Further, let $b''=b/(F/\hbar)$. Note that if $F>0$, $dk_x=|F/\hbar|d\tau$ and if $F<0$, $dk_x=-|F/\hbar|d\tau$. In either case, $\int_{-\infty}^{\infty}dk_x\to|F/\hbar|\int_{-\infty}^{\infty}d\tau$, since the limits of integration change sign with the sign of F according to the above substitution. Then, with $\beta\equiv F/\hbar$, the Green's function takes the form

$$G(y,y';x,x')=|\beta|\int_{-\infty}^{\infty}d\tau\frac{1}{2\pi}e^{i\beta\tau x}\int_{b''}^{\tau}d\tau'' e^{-i\beta\tau'' x'}\exp\left[-i\int_{\tau''}^{\tau}d\tau'\left[\beta\tau' v_x+\frac{\hbar\beta^2}{2M}\tau'^2+\beta x_0\right]\right]\int dk_y\frac{1}{2\pi}e^{ik_y[y-y'-v_y(\tau-\tau'')]} . \tag{A10}$$

The last factor is just $\delta(y-y'-v_y(\tau-\tau''))$. To ensure forward propagation, we want $G\to 0$ if $y<y'$. This requires $\tau>\tau''$. Hence, we take $b''=-\infty$ independent of the sign of F. Then the Green's function becomes

$$G(y,y';x,x')=|\beta|\int_{-\infty}^{\infty}d\tau\frac{1}{2\pi}e^{i\beta\tau x}\int_{-\infty}^{\tau}d\tau''e^{-i\beta\tau''x'}\exp-i\int_{\tau''}^{\tau}d\tau'\left[\beta\tau' v_x+\frac{\hbar\beta^2}{2M}\tau'^2+\beta x_0\right]\delta(y-y'-v_y(\tau-\tau''))\ . \tag{A11}$$

By construction, $\tau>\tau''$, so that the δ function in Eq. (A11) is zero unless $y>y'$. In this case, the τ'' integration is readily carried out to obtain

$$G(y,y';x,x')=\Theta(y-y')\frac{|\beta|}{v_y}\int_{-\infty}^{\infty}d\tau\exp\left[i\beta\tau x-i\beta\left[\tau-\frac{y-y'}{v_y}\right]x'\right]\exp\left[-i\int_{\tau-(y-y')/v_y}^{\tau}d\tau'\left[\beta\tau' v_x+\frac{\hbar\beta^2\tau'^2}{2M}+\beta x_0\right]\right]\ . \tag{A12}$$

The τ' integration in the phase is then carried out and yields

$$G(y,y';x,x')=\Theta(y-y')\frac{|\beta|}{v_y}\int_{-\infty}^{\infty}d\tau\frac{1}{2\pi}\exp\left[i\beta\tau(x-x')+i\beta\frac{y-y'}{v_y}x'\right]e^{i\phi(\tau)}\ , \tag{A13}$$

where the phase ϕ is given by

$$\phi(\tau)=-\beta v_x\tau\frac{y-y'}{v_y}+\frac{\beta v_x}{2}\left[\frac{y-y'}{v_y}\right]^2-\beta x_0\frac{y-y'}{v_y}-\frac{\hbar\beta^2}{2M}\tau^2\frac{y-y'}{v_y}+\frac{\hbar\beta^2}{2M}\tau\left[\frac{y-y'}{v_y}\right]^2-\frac{\hbar\beta^2}{6M}\left[\frac{y-y'}{v_y}\right]^3\ . \tag{A14}$$

It is convenient to make the substitution $k=\beta\tau$ in Eq. (A13). In this case, for $\beta>0$, $\int_{-\infty}^{\infty}d\tau\rightarrow\int_{-\infty}^{\infty}dk/|\beta|$. For $\beta<0$, $\int_{-\infty}^{\infty}d\tau\rightarrow\int_{\infty}^{-\infty}-dk/|\beta|=\int_{-\infty}^{\infty}dk/|\beta|$. The Green's function is then given by

$$G(y,y';x,x')=\frac{\Theta(y-y')}{v_y}\int_{-\infty}^{\infty}dk\frac{1}{2\pi}\exp\left[ik\left[x-x'-v_x\frac{y-y'}{v_y}\right]\right]\exp\left[-i\frac{\hbar k^2}{2M}\frac{y-y'}{v_y}-i\frac{\hbar\beta}{2M}k\left[\frac{y-y'}{v_y}\right]^2\right]$$
$$\times\exp\left[i\beta\frac{y-y'}{v_y}(x'-x_0)+i\frac{\beta v_x}{2}\left[\frac{y-y'}{v_y}\right]^2-i\frac{\hbar\beta^2}{6M}\left[\frac{y-y'}{v_y}\right]^3\right]\ . \tag{A15}$$

The form of Eq. (A15) can be improved somewhat by noting that in propagating the final-state amplitude, the integration over x' projects out the plane-wave component of wave vector k', where k' is the coefficient of $-x'$ in the phase which appears in the integrand above. With the substitution $k'=k-\beta[(y-y')/v_y]$, k may be eliminated in favor of the integration variable k'. Then, eliminating the $(')$ and using $\hbar\beta=F$, one obtains

$$G_F(y,y_2';x,x_2')=\frac{\Theta(y-y_2')}{v_y}\int_{-\infty}^{\infty}dk\frac{1}{2\pi}\exp\left\{ik\left[x-x_2'-v_x\frac{y-y_2'}{v_y}-\frac{F}{2M}\left[\frac{y-y_2'}{v_y}\right]^2\right]\right\}\exp\left[-i\frac{\hbar k^2}{2M}\frac{y-y_2'}{v_y}\right]$$
$$\times\exp\left[i\frac{F}{\hbar}\frac{y-y_2'}{v_y}(x-x_0)-i\frac{Fv_x}{2\hbar}\left[\frac{y-y_2'}{v_y}\right]^2-i\frac{F^2}{6\hbar M}\left[\frac{y-y_2'}{v_y}\right]^3\right]\ , \tag{A16}$$

which is identical to the Green's function given in Eq. (16) of the text.

APPENDIX B: DERIVATION OF THE INTEGRATED FINAL-STATE FLUX

To proceed, it is convenient to perform the x_2' integration in Eq. (15) first. From Eqs. (13) and (15) this requires evaluation of the integral

$$I\equiv\int dx_2'G_F(y,y_2';x,x_2')\exp\left[ik_1\left[x_2'-x_1'-v_x\frac{y_2'-y_1}{v_y}\right]\right]\exp\left[-i\frac{\hbar k_1^2}{2M}\frac{y_2'-y_1}{v_y}\right]\ . \tag{B1}$$

Using

$$\int dx_2' \frac{1}{2\pi} e^{i(k_1-k)x_2'} = \delta(k-k_1) \tag{B2}$$

yields

$$I = \frac{\Theta(y-y_2')}{v_y} \exp\left\{ik_1\left[x-x_1'-v_x\frac{y-y_1}{v_y}-\frac{F}{2M}\left[\frac{y-y_2'}{v_y}\right]^2\right]\right\}\exp\left[-i\frac{\hbar k_1^2}{2M}\frac{y-y_1}{v_y}\right]$$

$$\times\exp\left[-\frac{F}{\hbar}\frac{y-y_2'}{v_y}(x-x_0)-i\frac{Fv_x}{2\hbar}\left[\frac{y-y_2'}{v_y}\right]^2-i\frac{F^2}{6\hbar M}\left[\frac{y-y_2'}{v_y}\right]^3\right]. \tag{B3}$$

The k_1 integration required by Eqs. (15), (B3), and (13) is done next. This requires evaluation of the integral

$$I_1 = \int dk_1 \frac{1}{2\pi}\exp\left\{ik_1\left[x-x_1'-v_x\frac{y-y_1}{v_y}-\frac{F}{2M}\left[\frac{y-y_2'}{v_y}\right]^2\right]\right\}\exp\left[-i\frac{\hbar k_1^2}{2M}\frac{y-y_1}{v_y}\right] \tag{B4}$$

$$= \frac{\sqrt{\pi}}{2\pi}\exp\left\{+i\frac{Mv_y}{2\hbar(y-y_1)}\left[x-x_1'-v_x\frac{y-y_1}{v_y}-\frac{F}{2M}\left[\frac{y-y_2'}{v_y}\right]^2\right]^2\right\}\Big/\left[\frac{i\hbar}{2M}\frac{y-y_1}{v_y}\right]^{1/2}, \tag{B5}$$

where the observation point y is chosen downstream from the Raman region such that $y-y_1 \gg d$, and d is the radius of the Raman region. Since the Gaussian shape of the Raman regions constrains $y_2' \simeq y_1$ to within a distance d, the Θ function which appears in G_F can be taken equal to unity and the y_2' integration region formally extended to infinity. With this result the final-state amplitude takes the form

$$A_f(y,x) = -\frac{\Omega_{Ii}\Omega_{If}^*}{4v_y\left[\frac{\gamma_s}{2}-i\Delta\right]}\int dx_1' A_i(y_1,x_1')$$

$$\times\int_{-\infty}^{\infty} dy_2' \exp\left[-\left[\frac{y_2'-y_1}{d}\right]^2\right]$$

$$\times\exp\left[i\frac{F}{\hbar}\frac{y-y_2'}{v_y}(x-x_0)-i\frac{Fv_x}{2\hbar}\left[\frac{y-y_2'}{v_y}\right]^2-i\frac{F^2}{6\hbar M}\left[\frac{y-y_2'}{v_y}\right]^3\right]$$

$$\times\frac{\sqrt{\pi}}{2\pi}\exp\frac{\left\{+i\frac{Mv_y}{2\hbar(y-y_1)}\left[x-x_1'-v_x\frac{y-y_1}{v_y}-\frac{F}{2M}\left[\frac{y-y_2'}{v_y}\right]^2\right]^2\right\}}{\left[\frac{i\hbar}{2M}\frac{y-y_1}{v_y}\right]^{1/2}}, \tag{B6}$$

where the Rabi frequencies are evaluated at the peak of the Gaussian field distributions.

Our goal is to calculate the spatially integrated final-state flux at large distance downstream from the Raman region. The final-state atomic flux is proportional to $J = v_y |A_f(y,x)|^2$ for the case of a collimated atomic beam. The total signal is then $\dot{N} \propto \int\int dz\, dx\, J$, where the integrals extend across the atomic beam from $-\infty$ to ∞. In order to take the limit $y-y_1 \to \infty$ when the observation point is well outside the Raman region, it is necessary to do the infinite x-z integration *before* taking the large-y limit. In this way, all of the flux is included at each value of y. Since the amplitude is z independent, only the x integral need be explicitly done. Using dummy integration variables x_1', y_2' and x_1'', y_2'' for the final-state amplitude given in Eq. (B6) and its complex conjugate, the required integral is given by

$$\int_{-\infty}^{\infty}|A_f(y,x)|^2dx=\left|\frac{\Omega_{Ii}\Omega_{If}^*}{4v_y\left[\frac{\gamma_s}{2}-i\Delta\right]}\right|^2\int dx_1'\int dx_1''A_i(y_1,x_1')A_i^*(y_1,x_1'')$$

$$\times\frac{1}{4\pi}\int_{-\infty}^{\infty}dx\frac{\exp\left\{i\frac{Mv_y}{2\hbar(y-y_1)}\left[\left[x-x_1'-v_x\frac{y-y_1}{v_y}\right]^2-\left[x-x_1''-v_x\frac{y-y_1}{v_y}\right]^2\right]\right\}}{\frac{\hbar}{2M}\left|\frac{y-y_1}{v_y}\right|}$$

$$\times\int_{-\infty}^{\infty}\int_{-\infty}^{\infty}dy_2'dy_2''\exp\left[-\frac{(y_2'-y_1)^2+(y_2''-y_1)^2}{d^2}\right]\exp\left[i\frac{F}{\hbar}\frac{y_2''-y_2'}{v_y}(x-x_0)\right]$$

$$\times\exp\left[i\frac{Mv_y}{2\hbar(y-y_1)}\left\{\left[\frac{F}{2M}\left[\frac{y-y_2'}{v_y}\right]^2\right]^2-\left[\frac{F}{2M}\left[\frac{y-y_2''}{v_y}\right]^2\right]^2\right\}\right]$$

$$\times\exp\left\{-i\frac{Mv_y}{2\hbar(y-y_1)}2\frac{F}{2M}\left[(x-x_1')\left[\frac{y-y_2'}{v_y}\right]^2-(x-x_1'')\left[\frac{y-y_2''}{v_y}\right]^2\right]\right\}$$

$$\times\exp\left\{-i\frac{F^2}{6\hbar M}\left[\left[\frac{y-y_2'}{v_y}\right]^3-\left[\frac{y-y_2''}{v_y}\right]^3\right]\right\}. \tag{B7}$$

Note that the two terms proportional to $(Fv_x/2\hbar)[(y-y_2')/v_y]^2$ cancel in Eq. (B6), and hence do not appear in Eq. (B7).

At this point, the x integration is straightforward. We begin by rewriting Eq. (B7) in the form

$$\int_{-\infty}^{\infty}|A_f(y,x)|^2dx=\left|\frac{\Omega_{Ii}\Omega_{If}^*}{4v_y\left[\frac{\gamma_s}{2}-i\Delta\right]}\right|^2\int dx_1'\int dx_1''A_i(y_1,x_1')A_i^*(y_1,x_1'')$$

$$\times\int_{-\infty}^{\infty}\int_{-\infty}^{\infty}dy_2'dy_2''\exp\left[-\frac{(y_2'-y_1)^2+(y_2''-y_1)^2}{d^2}\right]\exp\left[-i\frac{F}{\hbar}\frac{y_2''-y_2')}{v_y}x_0\right]$$

$$\times\exp\left[i\frac{F^2[(y-y_2')^4-(y-y_2'')^4]}{8\hbar Mv_y^3(y-y_{1)}}\right]\exp\left[-i\frac{F^2[(y-y_2')^3-(y-y_2'')^3]}{6\hbar Mv_y^3}\right]$$

$$\times\exp\left[i\frac{F[x_1'(y-y_2')^2-x_1''(y-y_2'')^2]}{2\hbar v_y(y-y_1)}\right]$$

$$\times\exp\left\{i\frac{Mv_y}{2\hbar(y-y_1)}\left[\left[x_1'+v_x\frac{y-y_1}{v_y}\right]^2-\left[x_1''+v_x\frac{y-y_1}{v_y}\right]^2\right]\right\}I_x\ , \tag{B8}$$

where

$$I_x=\frac{1}{4\pi\frac{\hbar}{2M}\left|\frac{y-y_1}{v_y}\right|}\int_{-\infty}^{\infty}dx\exp\left[ix\left[\frac{F(y_2''-y_2')}{\hbar v_y}-\frac{Mv_y(x_1'-x_1'')}{\hbar(y-y_1)}-\frac{F[(y-y_2')^2-(y-y_2'')^2]}{2\hbar v_y(y-y_1)}\right]\right]$$

$$=\delta(x_1''-x_1'+\epsilon) \tag{B9}$$

and

$$\epsilon(y_2'',y_2')=\frac{F}{2Mv_y^2}[(y_2''-y_1)^2-(y_2'-y_1)^2]\ . \tag{B10}$$

With Eqs. (B8) and (B9), one obtains

$$\int_{-\infty}^{\infty}|A_f(y,x)|^2dx=\left|\frac{\Omega_{Ii}\Omega_{If}^*}{4v_y\left[\frac{\gamma_s}{2}-i\Delta\right]}\right|^2\int_{-\infty}^{\infty}\int_{-\infty}^{\infty}dy_2'dy_2''\exp\left[-\frac{(y_2'-y_1)^2+(y_2''-y_1)^2}{d^2}\right]$$
$$\times\exp\left[-i\frac{F}{\hbar}\frac{y_2''-y_2'}{v_y}x_0\right]\exp\left[i\frac{F^2}{\hbar Mv_y^3}\left[\frac{[(y-y_2')^4-(y-y_2'')^4]}{8(y-y_1)}-\frac{[(y-y_2')^3-(y-y_2'')^3]}{6}\right]\right]$$
$$\times\int dx_1'A_i(y_1,x_1')A_i^*(y_1,x_1'-\epsilon)\exp\left[i\frac{F[x_1'(y-y_2')^2-(x_1'-\epsilon)(y-y_2'')^2]}{2\hbar v_y(y-y_1)}\right]$$
$$\times\exp\left\{iMv_y\left[2\epsilon\left[x_1'+v_x\frac{y-y_1}{v_y}\right]-\epsilon^2\right]\Big/2\hbar(y-y_1)\right\}. \tag{B11}$$

In order to display explicitly the reality of the right-hand side of Eq. (B11), it is convenient to make the substitution $x_1'\rightarrow x_1'+(\epsilon/2)$. Equation (B11) then takes the form

$$\int_{-\infty}^{\infty}|A_f(y,x)|^2dx=\left|\frac{\Omega_{Ii}\Omega_{If}^*}{4v_y\left[\frac{\gamma_s}{2}-i\Delta\right]}\right|^2$$
$$\times\int_{-\infty}^{\infty}\int_{-\infty}^{\infty}dy_2'dy_2''\exp\left[-\frac{(y_2'-y_1)^2+(y_2''-y_1)^2}{d^2}\right]$$
$$\times\int dx_i'A_i\left[y_1,x_1'+\frac{\epsilon}{2}\right]A_i^*\left[y_1,x_1'-\frac{\epsilon}{2}\right]e^{i\phi(y_2',y_2'',x_1')}, \tag{B12}$$

where

$$\phi(y_2',y_2'',x_1')=\frac{F}{\hbar v_y}(y_2'-y_2'')x_0+\frac{F^2}{\hbar Mv_y^3}\left[\frac{[(y-y_2')^4-(y-y_2'')^4]}{8(y-y_1)}-\frac{[(y-y_2')^3-(y-y_2'')^3]}{6}\right]$$
$$+\frac{Fx_1'[(y-y_2')^2-(y-y_2'')^2]}{2\hbar v_y(y-y_1)}+\frac{F}{2\hbar v_y(y-y_1)}\frac{\epsilon}{2}[(y-y_2')^2+(y-y_2'')^2]$$
$$+\frac{Mv_y}{\hbar(y-y_1)}\left[x_1'+v_x\frac{y-y_1}{v_y}\right]\epsilon. \tag{B13}$$

Note that the right-hand side is invariant under complex conjugation if the substitution $y_2'\leftrightarrow y_2''$ is made (ϵ changes sign).

Next, we take advantage of the fact that the observation point y is chosen downstream from the Raman region at y_1, such that $y-y_1\gg y_2'-y_1\simeq d$. In this case, it is convenient to make the substitution $u_1=y_2'-y_1$ and $u_2=y_2''-y_1$. Then, $(y-y_2')^n-(y-y_2'')^n$, which appears in the phase ϕ can be written in the form $(y-y_1-u_1)^n-(y-y_1-u_2)^n$ and expanded exactly in powers of $(y-y_1)\gg u_i\simeq d$. Hence,

$$(y-y_2')^4-(y-y_2'')^4=-4(y-y_1)^3(u_1-u_2)+6(y-y_1)^2(u_1^2-u_2^2)-4(y-y_1)(u_1^3-u_2^3)+u_1^4-u_2^4,$$
$$(y-y_2')^3-(y-y_2'')^3=-3(y-y_1)^2(u_1-u_2)+3(y-y_1)(u_1^2-u_2^2)-u_1^3+u_2^3,$$
$$(y-y_2')^2-(y-y_2'')^2=-2(y-y_1)(u_1-u_2)+u_1^2-u_2^2, \tag{B14}$$
$$(y-y_2')^2+(y-y_2'')^2=2(y-y_1)^2-2(y-y_1)(u_1+u_2)+u_1^2+u_2^2,$$
$$\epsilon=\frac{F}{2Mv_y^2}(u_2^2-u_1^2).$$

These results are substituted into Eq. (B13) and terms are collected which are proportional to $(y-y_1)^n$ where n runs from $+2$ to -1. It is found that all terms vanish except for the one with $n=0$. The phase then takes the form

$$\phi(u_1,u_2,x_1')=-\frac{F}{\hbar v_y}(u_1-u_2)(x_1'-x_0)-\frac{Fv_x}{2\hbar v_y^2}(u_1^2-u_2^2)-\frac{F^2}{12\hbar Mv_y^3}(u_1-u_2)^3. \tag{B15}$$

The phase does not depend on the distance from the Raman region y_1 to the observation point y. This is reasonable, since the integrated flux at observation points well outside the Raman region ($y-y_1 \gg d$) should be independent of the observation position even when diffraction and acceleration are present. Note that the phase does not separate into two terms which are functions of u_1 and u_2 due to the cubic dependence on u_1-u_2. With Eq. (B15), the integrated final-state flux is given by

$$\int_{-\infty}^{\infty} dx\,|A_f(y,x)|^2 = \left| \frac{\Omega_{Ii}\Omega_{If}^*}{4v_y\left[\frac{\gamma_s}{2}-i\Delta\right]} \right|^2 \int dx_1' \int_{-\infty}^{\infty} du_1 \int_{-\infty}^{\infty} du_2 \exp\left[-\frac{u_1^2+u_2^2}{d^2}\right]$$
$$\times \exp\left[-i\left[\frac{F}{\hbar v_y}(u_1-u_2)(x_1'-x_0)+\frac{Fv_x}{2\hbar v_y^2}(u_1^2-u_2^2)+\frac{F^2}{12\hbar M v_y^3}(u_1-u_2)^3\right]\right]$$
$$\times A_i\left[y_1,x_1'+\frac{\epsilon}{2}\right] A_i^*\left[y_1,x_1'-\frac{\epsilon}{2}\right], \tag{B16}$$

where $\epsilon(u_1,u_2)$ is given in Eq. (B14).

Since the phase Eq. (B16) is dependent principally on the difference between u_1 and u_2 it is convenient to make the variable change $u_+ \equiv (u_1+u_2)/2$ and $u_- = u_1-u_2$. In this case, the Jacobian of the transformation is unity so that $du_1 du_2 = du_+ du_-$. Integration is over the entire plane. Substituting $u_1 = u_+ + (u_-/2)$ and $u_2 = u_+ - (u_-/2)$ into Eq. (B16), one obtains

$$\int_{-\infty}^{\infty} dx\,|A_f(y,x)|^2 = \left| \frac{\Omega_{Ii}\Omega_{If}^*}{4v_y\left[\frac{\gamma_s}{2}-i\Delta\right]} \right|^2 \int dx_1' \int_{-\infty}^{\infty} du_- \int_{-\infty}^{\infty} du_+ \exp\left[-\frac{u_-^2}{2d^2}\right] \exp\left[-\frac{2u_+^2}{d^2}\right]$$
$$\times \exp\left[-i\frac{Fv_x}{\hbar v_y^2}u_+u_-\right] \exp\left[-i\frac{F}{\hbar v_y}(x_1'-x_0)u_- - i\frac{F^2}{12\hbar M v_y^3}u_-^3\right]$$
$$\times A_i\left[y_1,x_1'-\frac{F}{2Mv_y^2}u_+u_-\right] A_i^*\left[y_1,x_1'+\frac{F}{2Mv_y^2}u_+u_-\right]. \tag{B17}$$

Equation (B17) gives the general result for the integrated flux in the final state in terms of the initial-state amplitude.

[1] See P. E. Martin, B. G. Oldaker, A. H. Miklich, and D. E. Pritchard, Phys. Rev. Lett. **60**, 515 (1988), and references therein.

[2] V. P. Chebotaev, B. Ya. Dubetsky, A. P. Kasantsev, and V. P. Yakovlev, J. Opt. Soc. Am. B **2**, 1791 (1985).

[3] C. Salomon, J. Dalibard, A. Aspect, H. Metcalf, and C. Cohen-Tannoudji, Phys. Rev. Lett. **59**, 1659 (1987).

[4] V. I. Balykin and V. S. Letokhov, Phys. Today **42** (4), 23 (1989).

[5] A. Aspect, E. Arimondo, R. Kaiser, N. Vansteenkiste, and C. Cohen-Tannoudji, Phys. Rev. Lett. **61**, 826 (1988).

[6] See, for example, W. D. Phillips, J. V. Prodan, and H. J. Metcalf, J. Opt. Soc. Am. B **2**, 1751 (1985).

[7] J. E. Thomas, Opt. Lett. **14**, 1186 (1989).

[8] See A. Anderson, S. Haroche, E. Hinds, W. Jhe, and D. Meshede, Phys. Rev. A **37**, 3597 (1988).

[9] See J. A. Yeazell, M. Mallalieu, and C. R. Stroud, Jr., Phys. Rev. Lett. **64**, 2007 (1990), and references therein.

[10] J. E. Thomas, P. R. Hemmer, S. Ezekiel, C. C. Leiby, Jr., R. H. Picard, and C. R. Willis, Phys. Rev. Lett. **48**, 867 (1982).

[11] M. Ozawa, Phys. Rev. A **41**, 1735 (1990).

[12] H. P. Huen, Phys. Rev. Lett. **51**, 719 (1983).